GEOPHYSICAL RESEARCH LETTERS, VOL. 22, NO. 3, PAGES 291-294, FEBRUARY 1, 1995

Simulation of proton radiation belt formation during the March 24, 1991 SSC

M. K. Hudson [1], A. D. Kotelnikov [1], X. Li [1], I. Roth [2], M. Temerin [2], J. Wygant [3], J. B. Blake [4], M. S. Gussenhoven [5]

Abstract. The rapid formation of a new proton radiation belt at $L \simeq 2.5$ following the March 24, 1991 Storm Sudden Commencement (SSC) observed at the CRRES satellite is modelled using a relativistic guiding center test particle code. The SSC is modelled by a bipolar electric field and associated compression and relaxation in the magnetic field, superimposed on a dipole magnetic field. The source population consists of both solar and trapped inner zone protons. The simulations show that while both populations contribute to drift echoes in the 20-80 MeV range, primary contribution is from the solar protons. Proton acceleration by the SSC differs from relativistic electron acceleration in that different source populations contribute and nonrelativistic conservation of the first adiabatic invariant leads to greater energization of protons for a given decrease in L. Model drift echoes and flux distribution in L at the time of injection compare well with CRRES observations.

Introduction

Protons were accelerated simultaneously with electrons to form new radiation belts following the Storm Sudden Commencement (SSC) of March 24, 1991 [see *Mullen et al.*, 1991, *Blake et al.*, 1992]. Previously [*Li et al.*, 1993], we showed that a simplified model of the SSC compression of the magnetosphere accelerates trapped outer zone electrons on a time scale short compared to their drift period. The model reproduced the drift echoes reported by *Blake et al.* [1992] from measurements made on the CRRES satellite, which fortuitously passed through the inner edge of the new radiation belt as it formed. In this Letter we show that the same pulse reproduces the proton drift echoes, including the double peaks reported by *Blake et al.*[1992], and the broad spectral peak observed above 20 MeV by the Protel instrument on CRRES [*Gussenhoven et al.*, 1993]. Two distinct ion source populations, solar protons and the inner zone protons, contribute to the new proton belt.

The CRRES satellite was located at a radial distance of $2.55 R_E$ geocentric near the equatorial plane and 0300 MLT at the time of the SSC [*Mullen et al.*, 1991, *Vampola and Korth*, 1992, *Blake et al.*, 1992], and observed the new radiation belt form in less than 150 seconds, along with the electric and magnetic field signatures of the SSC [*Wygant et al.*, 1994]. Modelling the SSC with a bipolar propagating electric field and associated compression and relaxation in the magnetic field, superimposed on a background dipole magnetic field, *Li et al.*[1993] followed the trajectories of 336,720 equatorially mirroring electron guiding centers using a relativistic test particle code which determines the guiding center velocity. We have speeded up the original code (25x) by vectorization and replacing the energy conservation equation ((2) in *Li et al.*[1993]) with the adiabatic change in energy along the ion trajectory. The magnetospheric compression is modelled by an induction electric field exactly as in *Li et al.*[1993]. Faraday's law determines the magnetic field, which is purely compressional in the model, but has an azimuthal as well as radial gradient, while two exponentials describe inbound and outbound pulses which approximate compression and relaxation of the magnetosphere.

Figure 1 shows the maximum azimuthal electric field wavefront (a) inbound and (b) outbound at successive times. At t=0 the pulse maximum is at about 25 R_E at ϕ_0, and it reaches 10, 1.05 and 10 R_E again at 48, 76 and 105 seconds, respectively. The pulse is assumed to strike the magnetopause at 1500 MLT, motivated by conclusions drawn from the arrival times of the first newly accelerated electrons and protons observed at CRRES [*Blake et al.*, 1992], and the electron simulations of *Li et al.*[1993]. The initial dipolar field remains partially compressed after the pulse leaves the system. In the model, all reflection occurs at the ionosphere, although partial reflection will occur from various gradients within the magnetosphere. Also, the pulse velocity is constant in the model, and taken to be a characteris-

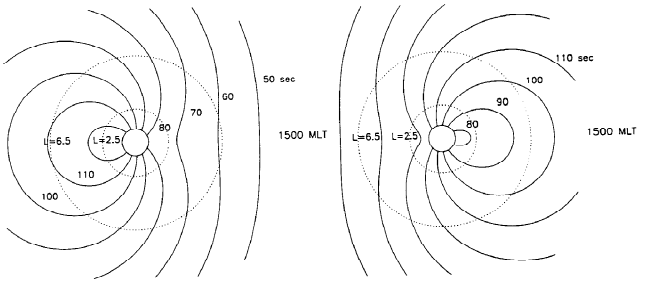

Figure 1. Maximum azimuthal electric field wavefront at successive times. a) Shows inbound and b) shows outbound pulse inside L=12 with times labeled from beginning of simulation (t=0) when pulse is at about 25 R_E. Dotted L=2.5 and L=6.5 contours are labeled.

[1] Dartmouth College, Hanover, New Hampshire
[2] University of California, Berkeley, California
[3] School of Physics and Astronomy, University of Minnesota
[4] The Aerospace Corporation, Los Angeles, California
[5] Phillips Laboratory, Hanscom AFB, Massachusetts

Paper number 95GL00009
0094-8534/95/95GL-00009$03.00

tic fast mode speed in the outer magnetosphere. Actually, the velocity will increase radially inward from the magnetopause with increasing magnetic field strength, then decrease at the plasmapause, rising again toward the ionosphere as the magnetic field gradient dominates over the plasma density gradient in the Alfvén speed [*Moore et al.*, 1987]. The model used is optimized to reproduce the particle signatures observed at CRRES [*Li et al.*, 1993], and is not expected to accurately model the reflected pulse outside the plasmapause.

Simulation Results

We have followed 683,760 proton trajectories for a minimum of 180 seconds, or well after the model pulse has left the magnetosphere. We have assumed that solar protons constitute a significant source population because of their substantial flux in both CRRES and GOES data [*Mullen et al.*, 1991, *Gussenhoven et al.*, 1994] preceding the sudden commencement. Figure 2a shows the proton differential number flux perpendicular to the local magnetic field direction, measured by Protel on CRRES and interpolated between discrete energy channels, for the descending leg of the orbit in which the SSC occurred. Protel measured differential proton flux in 24 energy channels from 1-100 MeV [*Violet et al.*, 1993]. The SSC appears as a discontinuity in flux at L=2.55. The solar protons are the broad swath of particles at high L values. Their penetration depths depend on energy. The stable proton radiation belt appears in the lower left corner. This belt has been modelled with a power law index of W^{-5} inside L=4, which is an average value taken from NASA models [*Spjeldvik and Rothwell*, 1985], and a W^{-3} power law outside L=4, to match fluxes measured by the lowest energy channels of Protel near geosynchronous orbit [*Gussenhoven et al.*, 1993]. Solar protons are modelled between L=6-9 with a power law of the form $W^{0.3}$ over the energy range $2 < W < 25$ MeV; for $4 \leq L < 6$ the minimum or cutoff energy is $W_0 > 2(6/L)^3$, to simulate the greater penetration of higher energy solar protons. All source protons are uniformly distributed in longitude ϕ, while a radial envelope of the form $S(L) = (1 - 4/L)^2$ for $4 \leq L < 6$ and uniform for $L > 6$ is applied. A radial envelope of the form $S(L) = 10^{-0.9L}(4/L - 1)^2$ is applied to inner zone protons inside L=4. The total source population, as modelled, is shown in Figure 2b. It compares well with the measured values pre-SSC.

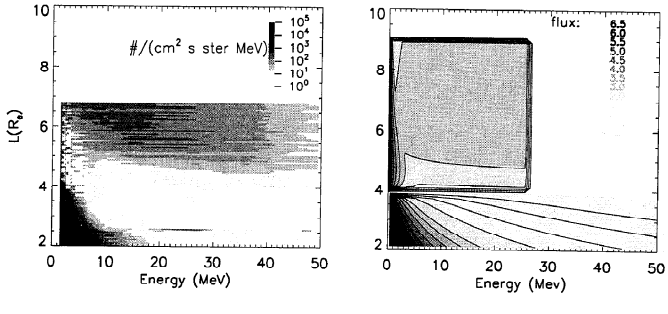

Figure 2. a) Proton differential number flux at 90 degree pitch angle, measured by Protel on CRRES and interpolated between discrete energy channels, for orbit in which SSC occurred (data accumulated over 5 hours from apogee to perigee). b) Model source populations. Darkest contours model inner zone. Relative flux is plotted on same scale as Figure 4, without incorporation of detector geometric factors.

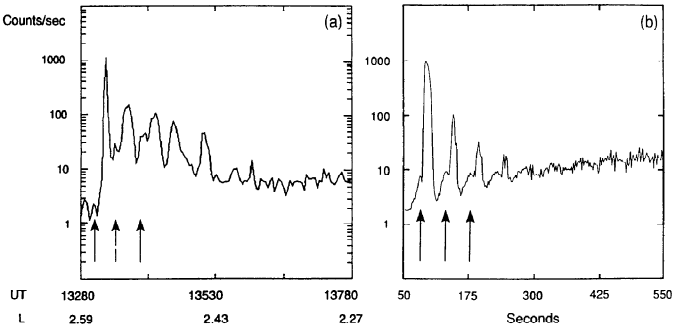

Figure 3. a) Omnidirectional flux measured by 20-80 MeV proton channel of Aerospace instrument on CRRES [*Blake et al.*, 1992]. b) Simulated proton drift echoes using same pulse parameters as *Li et al.* [1993]. Source population is shown in Figure 2b. Simulation includes motion of spacecraft and Aerospace proton instrument response as function of energy, with 23.5 MeV low energy cutoff. Drift echos beyond t=180 seconds are obtained by extrapolation of drift motion. Inner zone drift echo peaks are indicated by arrows.

Proton drift echoes are produced, as shown in Figure 3, due to interaction with the pulse over a limited range of drift longitude, which produces drift phase bunching. Omnidirectional flux measured by the Aerospace instrument on CRRES in the energy range 20-80 MeV is shown in panel (a) [*Blake et al.*, 1992]. Secondary drift echoes indicated by arrows are shifted relative to the main peaks. Simulation results using the model solar proton and inner zone populations described above are shown in panel (b). The simulation includes motion of the spacecraft and the instrument response as a function of energy, with a 23.5 MeV low energy cutoff. This cutoff determines the drift echo period, given the energy spectrum obtained from the simulation (Figure 4a). Drift echoes beyond t=180 seconds are obtained under the assumption of no further hydromagnetic wave interaction, although there are subsequent relaxation oscillations of the magnetosphere in the data [*Wygant et al.*, 1994]. We find that the secondary drift echo peaks become more prominent as the spacecraft moves inward. They are due to inner zone protons, from inside L=4, whereas the primary peaks are due to solar protons from beyond L=4. The secondary drift echoes due to the inner zone preceed the solar proton peaks because proton ring distributions of the same initial magnetic moment from higher L_0 do not cross those from lower L_0, so phase bunched inner zone protons reach the detector first. This effect is also evident in the low energy channels of Protel, 1-2 MeV in width, below 20 MeV [*Hudson et al.*, 1994]. We have also simulated the higher energy channel of the Aerospace proton instrument on CRRES, 50-110 MeV [*Blake et al.*, 1992], and find that the flux at these energies at $L < 2.6$ is entirely due to inner zone protons.

In Figure 4a we have plotted the relative flux vs. energy and L shell in the simulation, after the pulse has left the system and the protons have undergone at least

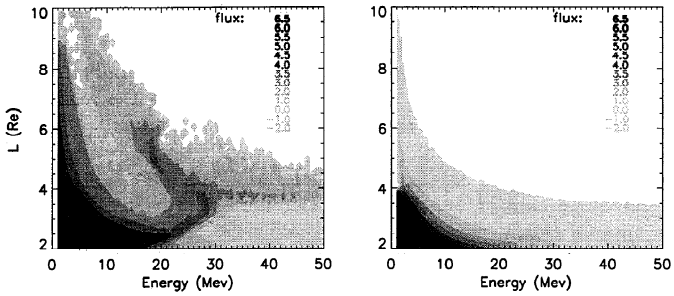

Figure 4. a) Relative proton flux vs. energy and L shell, averaged over ΔL=0.1 and ΔW=0.5 MeV, parameters as in Figure 3. (b) contribution from protons initially at $L \leq 4$.

one drift period. The results are plotted in (a) for the combined inner zone and solar proton source, while (b) shows the contribution from protons initially at $L \leq 4$. Examining the solar proton source contribution shows that the rise in the input solar proton source spectrum in Figure 2b is moved inward in L, contributing most to flux above 10 MeV. The protons in the spectral peak around 25 MeV at L=3, for example, are due to solar protons. The inner zone contributes the monotonically decreasing energy spectrum which is predominant below L=2.25 in (a). The upward rising plume between L=4-6 from 18-30 MeV is due to proton interaction with the outbound pulse, which removes energy from protons accelerated by the inbound pulse. Simply reducing the outbound pulse amplitude shifts these protons to higher energy and lower L [*Hudson et al.*, 1994]. However, the present model is not expected to be accurate outside $L \simeq 4$ because of neglect of partial reflection from the plasmapause.

CRRES Protel data from the outbound pass, two hours after the SSC, shows an enhancement of the inner zone population between L=2 and 3.5, as seen in the simulation. At this time, the new radiation belt extends to higher energies than in the simulation, with a double belt structure which peaks in the energy range 20-40 MeV at $L \sim 2.75$ and 15-30 MeV at $L \sim 3.5$. The spectrum seen in Figure 2a at the time of injection is more narrowly peaked in energy about 25 MeV, as in the simulation.The double belt structure seen on the outbond pass suggests additional acceleration, perhaps by secondary solar wind impulses apparent in ground magnetograms subsequent to the SSC.

In analogy with the electrons, where most acceleration occurs over the longitude sector 1500-1800 MLT for a pulse striking the magnetopause at 1500 MLT, protons gain the most energy over the longitude sector 1200-1500 MLT where the radial component of the pulse $\nabla \mathbf{B}_w$ drift adds to the $\mathbf{E}_w \times \mathbf{B}$ drift inward. It is useful to isolate the effect of the inbound pulse on individual protons which contribute to the new radiation belt. An example of three accelerated proton trajectories is shown in Figure 5 for the same pulse parameters as Figure 3, without the outbound pulse. The three protons were chosen from ring distributions in L at L_0=9, 7 and 5, with $M_r = 1.25 \times 10^3$ MeV/G, to be those which have the smallest final L, $L_f \simeq 2.5$, hence are most accelerated. There is a slight spread in L_f not evident, because particles of a given M_r which come from a higher L_0 have a higher L_f, as noted by Li et al. [1993] for electrons. However, the compression in L is significant, from ΔL_0=5 to $\Delta L_f \simeq .2$, and contributes to the flux and localization in L of the most accelerated particles. Figure 5 shows that all three protons were accelerated in the longitude sector where the pulse amplitude is maximum. The proton initially at $L_0 = 9$ experiences a reversal in azimuthal drift because the azimuthal component of the $\nabla \mathbf{B}_w$ drift due to the pulse opposes and is larger than the dipole field drift at large L. This partial cancellation or reversal of the azimuthal drift allows a proton to spend longer than otherwise in the longitude sector where $\nabla \mathbf{B}_w$ and $\mathbf{E}_w$ produce inward radial motion.

In order to achieve significant acceleration, a proton must satisfy two conditions: (a) it must encounter the pulse when the electric field amplitude is large, so the phase of the pulse along the particle trajectory must be small, and (b) it must stay with the pulse for a sufficiently long time, so the change in phase of the pulse along its trajectory must be small. When the reflected pulse is included in the simulations of Figure 5, the outbound pulse removes some energy on average from the newly accelerated protons. However, the two conditions (a) and (b) above are not necessarily optimized for the reflected pulse phase, so there is a population which remains at $L \simeq 2.5$ after the outbound pulse has left.

Conclusion

The simulations reported here reproduce several important features of the new proton belt which resulted from the March 24, 1991 SSC. Our results have shown that the double peaked proton drift echoes reported by *Blake et al.*[1992] result from two distinct source populations, solar protons which populate the magnetosphere into $L \simeq 4$ with increasing flux up to and including the time of the SSC, and the pre-existing inner zone. The broad spectral peak observed above 20 MeV by the Protel instrument on CRRES is due primarily to solar protons. Subtracting out the inner zone in Figure

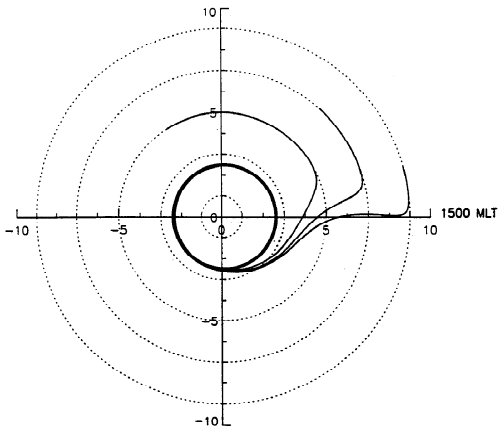

Figure 5. Trajectories of three protons interacting with inbound pulse only. Three protons were chosen from ring distributions in L at L_0=9, 7 and 5, with $M_r = 1.25 \times 10^3$ MeV/G, to be those most accelerated, with smallest final $L \simeq 2.5$. All arrive at $L \simeq 2.5$ with 25 MeV, starting at $L_0 = 9$ (.5 MeV), 7 (1 MeV) and 5 (3 MeV).

4b from Figure 4a shows the energy dependence of the flux peak as a function of L for solar protons, which approximately follows conservation of M_r, corresponding to $W \sim L^{-3}$ for nonrelativistic protons, vs. $W \sim L^{-3/2}$ for relativistic electrons [*Li et al.*, 1993]. Thus protons gain more energy than electrons for a given change in L. There is a smaller change in L, hence energy, for the inner zone contribution in Figure 4b. The source populations for protons are distinct from the source population for electrons in the simulation of *Li et al.* [1993], where the new radiation belt electrons came from a W^{-8} trapped outer zone source, with the most energetic particles coming from highest L values.

The results shown here, together with those of our previous Letter [*Li et al.*, 1993], show that ion and electron radiation belts can be created in tens of seconds due to the interaction of an interplanetary shock wave with the magnetosphere. The rate at which particles gain energy within the magnetosphere is truly amazing. Indivdual ions and electrons gained tens of MeV during their brief interaction. This event suggests that important consideration should be given to the role of interplanetary shocks and associated SSC's and Sudden Impulses (SI's) in creating the semi-permanent radiation belts. Future work will examine this event in more detail by (1) using an improved field model obtained from self-consistent MHD simulations [*Lyon et al.*, 1994]; (2) including non-equatorially mirroring particles, and (3) including the effects of hydromagnetic oscillations which persisted after the main SSC pulse [*Wygant et al.*, 1994]. In addition, future studies should address the redistribution of proton and electron flux in L during the several days of activity following the SSC [*Mullen and Gussenhoven,* 1994], as well as the decay of the new radiation belts which persisted through the end of the CRRES mission in October 1991, still observed by SAMPEX in 1993 [*Looper et al.*, 1994].

Acknowledgments. We would like to express our appreciation to J. Albert and G. Ginet, Phillips Laboratory, for helpful discussions, J. Lyon and E. Witt of Dartmouth for discussion and code suggestions. Work at Dartmouth was supported by AFOSR grant F49620-93-1-0101, at Dartmouth and Berkeley by NASA grant NAG 5-1098, at the Aerospace Corporation by the Air Force under contract F04701-88-C-0089 and at Berkeley by LACOR contract LANL UC 94-1-A-210 and by Air Force contracts F19628-87-K0016 and F19628-92-K0009. Computations were performed on the SDSC and PSC Crays.

References

Blake, J. B., W. A. Kolasinski, R. W. Fillius, and E. G. Mullen, Injection of electrons and protons with energies of tens of MeV into $L < 3$ on March 24, 1991, *Geophys. Res. Lctt., 19,* 821, 1992.

Ginet, G. P., W. J. Burke, and J. Albert, An analysis of electron energization seen in simulations of the March 24, 1991 SSC, *EOS Trans. Am. Geophys. Union, 75,* 305, 1994.

Gussenhoven, M. S., E. G. Mullen, M. D. Violet, C. Hein, J. Bass, and D. Madden, CRRES high energy proton flux maps, *IEEE Trans. Nucl. Sci., 40,* 1450, 1993.

Gussenhoven, M. S., E. G. Mullen, M. D. Violet, Solar particle events as seen as CRRES, *Advances in Space Res., 14,* 619, 1994.

Hudson, M. K., A. Kotelnikov, X. Li, I. Roth, M. Temerin, J. Wygant, J. B. Blake, and M. S. Gussenhoven, Modelling formation of new radiation belts and response to ULF oscillations following March 24, 1991 SSC, *EOS Trans. Am. Geophys. Union, 75,* 538, 1994.

Li, X., I. Roth, I., M. Temerin, J. R. Wygant, M. K. Hudson, and J. B. Blake, Simulation of the prompt energization and transport of radiation belt particles during the March 24, 1991 SSC, *Geophys. Res. Lett., 20,* 2423, 1993.

Looper, M. D., J. Blake, R. Mewaldt, J. Cummings, and D. Baker, Observations of the remnants of the ultrarelativistic electrons injected by the strong SSC of 24 March 1991, *Geophys. Res Lett., 21,* 2079, 1994.

Lyon, J.G., M.K. Hudson, J.A. Fedder, and C.C. Goodrich, Global MHD simulation of the March 24, 1991 SSC, *EOS Trans. Am. Geophys. Union, 75,* 539, 1994.

Moore, T. E., D. L. Gallagher, J. L. Horwitz, and R. H. Comfort, MHD wave breaking in the outer plasmasphere, *Geophys. Res. Lett., 14,* 1007, 1987.

Mullen, E.G., M.S. Gussenhoven, K. Ray, and M. Violet, A double-peaked inner radiation belt: cause and effect as seen on CRRES, *IEEE Trans. Nucl. Sci., 38,* 1713, 1991.

Mullen, E.G., and M.S. Gussenhoven, Additional dynamics of the second proton belt formation during the March 1991 magnetic storm, *EOS Trans. Am. Geophys. Union, 75,* 304, 1994.

Northrop, T. G., *The adiabatic motion of charged particles.* Interscience Publishers, New York, 1963.

Spjeldvik, W.N. and P.L. Rothwell, The Radiation Belts, Chapter 5 in *Handbook of Geophysics and the Space Environment,* edited by A.S. Jursa, AFGL, Hanscom AFB, Massachusetts, 1985.

Vampola, A. K., and A. Korth, Electron drift echoes in the inner magnetosphere, *Geophys. Res. Lett., 19,* 625, 1993.

Violet, M. D., K. Lynch, R. Redus, K. Riehl, E. Boughan, and C. Hein, Proton telescope (Protel on the CRRES spacecraft, *IEEE Trans. Nuc. Sci., 40,* 242, 1993.

Wygant, J. R., F. Mozer, M. Temerin, J. B. Blake, N. Maynard, H. Singer, and M. Smiddy, Large amplitude electric and magnetic field signatures in the inner magnetosphere during injection of 15 Mev electron drift echoes, *Geophys. Res. Lett., 21,* 1739, 1994.

(received Nov. 3, 1994; accepted Dec. 5, 1994.)